

DQPSK Demodulation Using Integrated Silicon Ring Resonators

L. Xu, C. Li, X. Chen and H. K. Tsang

Dept. of Electronic Engineering, the Chinese University of Hong Kong, Shatin, N. T., Hong Kong

Phone:+852 26098254 Fax:+852 26035558 Email: hktsang@ee.cuhk.edu.hk

Abstract—We experimentally demonstrated an ultra-small 20Gb/s differential quadrature phase-shift keying (DQPSK) demodulator using silicon based microring resonators. The double-waveguide microring resonators enable detection of I and Q signals as well as inverted I and Q signals.

Keywords—Differential quadrature phase-shift keying (DQPSK); silicon integration

I. INTRODUCTION

Phase-shift keying provides enhanced sensitivity and tolerance to fiber nonlinearities when compared with on-off-keying (OOK). Differential quadrature phase-shift keying (DQPSK) doubles the spectral efficiency when compared with binary formats such as OOK or differential phase-shift keying (DPSK). The most common approach for DQPSK demodulation employs a Mach-Zehnder delay interferometer (MZDI) for demodulation of each quadrature [1], followed by balanced detection. Optical frequency discriminator with direct detection is also an alternative approach [2]. DPSK demodulation based on a frequency discriminator implemented with a silicon microring resonator was recently demonstrated [3] to operate over a wider range of bit rates than the conventional MZDI approach. Zhang, et al [4] recently analyzed the performance of DQPSK demodulation using microring resonators. Compared to the MZDI approach, microring structures occupy a much smaller chip area and are thus easy to stabilize thermally and can be integrated with other devices such as waveguide photodetectors.

In this paper, we report the performance of a pair of integrated silicon microring resonators for 20 Gb/s DQPSK demodulation. The testing of the frequency discriminator employed 10Gb/s DPSK for each quadrature channel, and we showed that tuning of the resonator frequency to match the requirements of DQPSK demodulation may be achieved by localized optical heating of each resonator.

II. DEVICE DESIGN

The integrated microring resonators were fabricated at IMEC on silicon-on-insulator (SOI) wafer with a 0.22- μm thick top silicon layer and a 2- μm thick buried oxide (BOX) layer. The waveguides were nominally 500nm wide and the device layout was defined by 193nm-deep-UV photolithography, and transferred onto the device layer by dry etching. The entire device was clad with a 0.75- μm -thick high density plasma (HDP) oxide. Fig.1 shows the top-view scanning electron micrograph of the fabricated microring

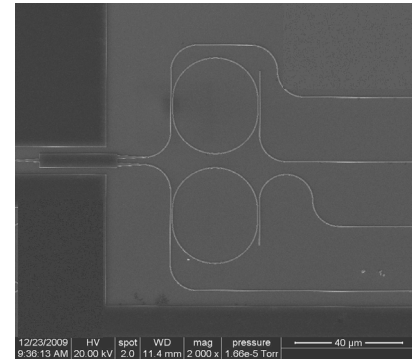


Fig.1 Top view of the device

device. The racetrack microring arc radius is 15 μm , and the straight interaction length is 8 μm . The fabricated air-gap spacing g between the ring and the waveguide is about 200nm.

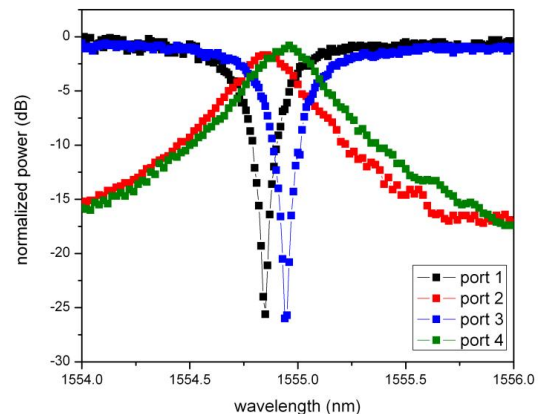


Fig.2 Measured TE-polarized through-port and drop-port spectra of the fabricated silicon microring resonators.

The spectra of TE-polarized light at the through port and drop port, measured using a narrow linewidth tunable laser with 0.01 nm spectral resolution, are shown in Fig.2. It is found that the transmitted power at the on-resonance wavelength drops by more than 25 dB with respect to that of the off-resonance wavelengths. The quality factor (Q) for both resonators were measured to be about 6500. Input and output coupling to the microresonators were via integrated fiber grating couplers [5] coupling to single mode optical fibers orientated at about ten degrees off-vertical.

III. EXPERIMENT

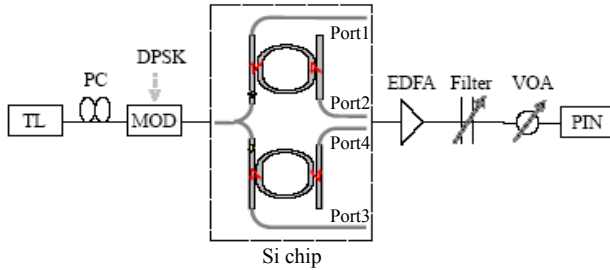


Fig. 3 Experimental set up. TL: tunable laser; MOD: modulator; VOA: variable optical attenuator; PIN: Pin diode

The experimental setup is shown in Fig.3. A CW light at the wavelength of 1554.85/1554.94nm was generated by a tunable laser (HP 8168F) with 0.001nm tuning step and was tuned exactly to the resonance of one resonator. It was then phase modulated with the data generated from a pseudo-random binary sequence (PRBS) pattern generator with a pattern length of $2^{31}-1$ at 10Gb/s data rate. The generated DPSK signal was coupled into a microring resonator through input port of 1x2 MMI and then coupled out from output port 1/port 3, which extracted the AMI format from the DPSK spectrum for detection.

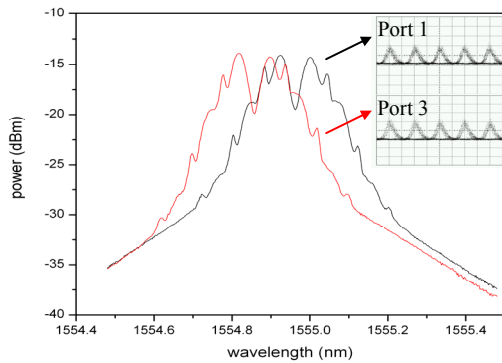


Fig. 4 The spectra after filtering and respective eye diagrams

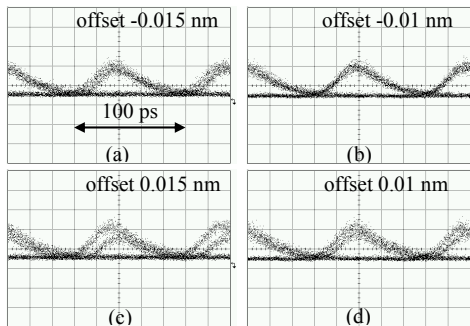


Fig. 5 Eye diagrams of demodulated signal at different offset frequencies

Fig.4 shows spectra after demodulation measured with a nominal 0.01nm 3dB-bandwidth spectral resolution optical spectrum analyzer. The inset pictures show clean and open demodulated eye diagrams at 10Gb/s. Wavelength detuning against the resonance wavelength was investigated for port 1 shown in Fig. 5. Here a negative detuning is defined as tuning

the signal towards shorter wavelength while positive detuning means tuning towards longer wavelength. Fig.5(a)-(d) show demodulated eye diagrams of negative detuning of -0.015 nm to positive detuning of 0.015 nm. It is shown that the negative detuning has a better tolerance for signal demodulation.

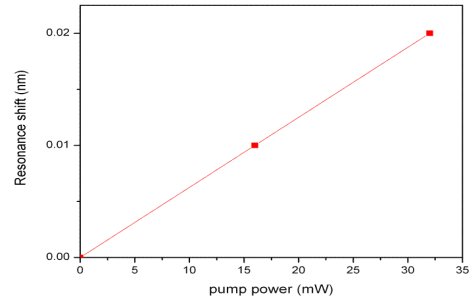


Fig. 6 Resonance shift against injected pump power

Precise tuning of the two microrings may be carried out using electrical wire heaters. However for this proof-of-principle experiment, we used the local heating from the absorption of 980 nm wavelength light to tune the resonator's refractive index. The absorption of light produces free carriers (reduces the refractive index) and local heating (increases the refractive index). It is observed that the thermo-optic effect is the larger effect since the resonant wavelength shifts to longer wavelength as shown in Fig.6. It is thus possible to tune the resonance separation of the two rings match the required $\frac{1}{4}$ symbol rate for DQPSK demodulation (2.5 GHz separation for 20 Gb/s DQPSK demodulation) [4].

IV. CONCLUSION

We experimentally demonstrated a silicon integrated microring resonator device for DQPSK demodulation. The performance was studied using DPSK for each channel for proof-of-principle. We show that the resonance separation between I and Q channel can be tuned to match the $\frac{1}{4}$ symbol rate for DQPSK demodulation.

Acknowledgments: We thank ePIXfab (www.epixfab.eu) for device fabrication.

References

- [1] Y. K. Lizé, M. Faucher, É. Jarry, P. Ouellette, É. Villeneuve, A. Wetter, and F. Séguin, "Phase-tunable low-loss, S-, C-, and L-band DPSK and DQPSK demodulator," *IEEE Photon. Technol. Lett.*, vol. 19, no. 3, pp.1886–1888, 2007.
- [2] C. C. Chien, Y. H. Wang, I Lyubomirsky, and Y. K. Lizé, "Experimental Demonstration of Optical DQPSK Receiver Based on Frequency Discriminator Demodulator", *J. Lightw. Technol.* vol. 27, no. 19, pp. 4228-4232, 2009
- [3] L. Xu, C Li, C. Y. Wong, and H. K. Tsang, "Optical Differential-Phase-Shift-Keying Demodulation Using a Silicon Microring Resonator", *IEEE Photon. Technol. Lett.*, vol. 21, no. 5, 2009
- [4] L. Zhang, J. Y. Yang, Y. C. Li, M. P. Song, R. G. Beausoleil, and A. E. Willner, "Monolithic modulator and demodulator of differential quadrature phase-shift keying signals based on silicon microrings", *Optics Lett.*, vol. 33, no. 13, pp. 1428-1430, 2008
- [5] D. Taillaert, F. V. Laere, M. Ayre, W. Rogaerts, D. V. Thourhout, P. Bienstman and R. Baets, "Grating couplers for coupling between optical fiber and nanophotonic waveguide", *Jap. J. Appl. Phys.*, vol. 45, pp. 6071-6077, 2006.